

ULTIMATE PERFORMANCE OF RELATIVISTIC ELECTRON COOLING AT FERMILAB*

A. Shemyakin[#] and L. R. Prost, FNAL, Batavia, IL 60510, U.S.A.

Abstract

Fermilab's Recycler ring employs a 4.3 MeV, 0.1A DC electron beam to cool antiprotons for accumulation and preparation of bunches for the Tevatron collider. The most important features that distinguish the Recycler cooler from other existing electron coolers are its relativistic energy, a low longitudinal magnetic field in the cooling section, ~100 G, and lumped focusing in the electron beam lines. The paper summarizes the experience of designing, commissioning, and optimizing the performance of this unique machine.

INTRODUCTION

An electron cooler was envisioned as an important part of the Recycler ring [1]. The main cooler parameters (Table 1) were chosen to satisfy the Recycler goals: store antiprotons coming from the Accumulator, prepare bunches for Tevatron shots, and "recycle" particles left over from Tevatron stores. Because of the longitudinal injection scheme of the Recycler, the main emphasis was made on longitudinal cooling. Note that later changes, most notably the decision not to "recycle" antiprotons from the Tevatron and the lower than predicted emittances of the bunches coming from the Accumulator, relaxed the operational requirements for the cooler.

Table 1: Parameters of the cooler

Parameter	Unit	Design	Operation
Electron energy	MeV	4.33	4.33
Beam current, DC	A	0.5	0.1
Magnetic field in the cooling section	G	100-200	105
Beam radius in the cooling section	mm	~5	~2
Pressure	nTorr	1	0.3
Total length of the beam line	m	90	90

As soon as the electron beam could be reliably sustained in 2005, relativistic electron cooling was demonstrated [2] and within days was put into operation. Since then, electron cooling significantly contributed to a several-fold increase of the Tevatron luminosity until the end of operation in October 2011.

In this paper, we discuss the choice of the cooler's scheme and its implementation, describe the setup and cooling measurement procedures, and present the ultimate results .

CHOICE OF THE SCHEME

The scenario of using the Recycler electron cooler [3] assumed typical cooling times of tens of minutes.

Estimations showed that at a reasonable electron current (~0.5A) it could be achieved without using the benefits of a strong magnetic field in the cooling section. Such "non-magnetized" approach was a clear deviation from the tested way of building coolers, creating serious questions about the stability of the electron beam transport and ability to provide low transverse electron velocities in the cooling section. On the other hand, estimations of the budget available and time needed to develop an "all-magnetized" version of the cooler and contribute to Fermilab's Run II showed that it was not realistic.

Nevertheless, simply leaving a lumped focusing in the cooling section to counteract the electron beam's space charge looked dangerous because of beam interactions with the residual ions background and with the vacuum chamber walls [4]. However, it was realized that it is theoretically possible to transport an electron beam from one solenoid to another through a lumped-focusing section without excitation of additional angles with the appropriate choice of optics for this section [5]. As a result, a novel scheme was chosen where the electron gun and the cooling section are both immersed in a longitudinal magnetic field but the beam focusing in between is provided by separate solenoidal lenses.

Applicability of such scheme is critically dependent on the magnetic flux in the cooling section. When a beam with no transverse velocities inside a solenoid exits into a free space, conservation of the canonical angular momentum results in a coherent angular rotation of the beam. In the paraxial ray equation, it is equivalent to the addition of an effective normalized emittance [5]

$$\varepsilon_{B,eff} = \frac{e\Phi}{2\pi m_e c^2}, \quad (1)$$

where $\Phi = B_{CS} R_{CS}^2$ is the magnetic flux through the beam cross section in the solenoid, e and m_e are the electron charge and mass, and c is the speed of light. As in the case with a real emittance, the beam transport with lumped focusing is possible only if this emittance is low enough. For example, a transport channel for $\gamma = 10$ with a typical beam radius of ~1 cm and the beta-function of ~1 m to bring the beam into a cooling section at the radius of $R_{CS} \sim 1$ cm limits the solenoid magnetic field to ~300G. To use lumped focusing during acceleration (i.e. at lower γ), the magnetic flux had to be decreased in comparison with this example by limiting both the beam size and the magnetic field strength in the cooling section down to $R_{CS} = 2 - 4$ mm and $B_{CS} = 100 - 200$ G.

Because of the large (reactive) beam power required in the cooling section, ~1 MW, using the energy recovery

scheme, standard for electron coolers, is even more important for the Recycler cooler.

SETUP

Elevation views of the electron cooler are shown in Figure 1.

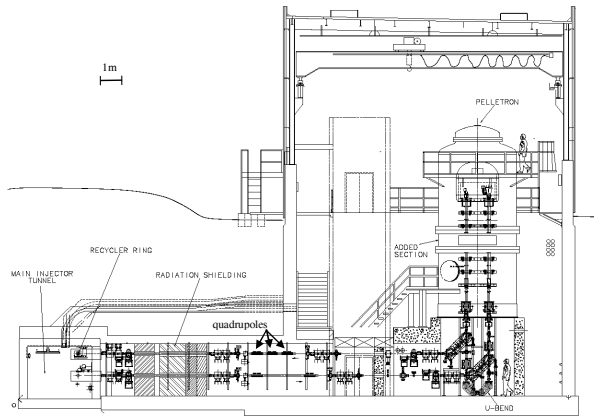


Figure 1a: Elevation view showing the Pelletron, the transfer lines passing through the connecting enclosure to the Recycler ring, and the cross-section of the Main Injector (MI) tunnel which houses the Recycler ring.

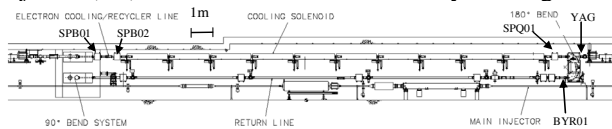


Figure 1b: Elevation view of the MI tunnel showing the 90°-bend system which injects the electron beam from the transfer line into the Recycler ring, the cooling section of Recycler, the 180°-bend system which extracts the electron beam from the Recycler, and the return line.

Electrons are emitted by a thermionic cathode, accelerated inside an electrostatic accelerator, Pelletron [6], and transported through a beam “supply” line to the cooling section where they interact with antiprotons circulating in the Recycler. After separation of the beams by a 180 degree bend, electrons move through the “return” beam line out of the tunnel, and then through a “transfer” line back to the Pelletron. Inside the Pelletron, the electron beam is decelerated in the second (“deceleration”) tube and is absorbed in a collector at the kinetic energy of 3.2 keV. The main ideas for a low-halo gun are described in [7], and performance of the collector is presented in [8].

The vacuum chamber is pumped down by ion and titanium sublimation pumps. The diameter of the vacuum pipe is 47 mm in the cooling section and 75 mm in the beam lines, where the aperture is limited by the BPM's inner diameter also of 47 mm. The typical pressure is 0.3 nTorr (mainly hydrogen).

When both main bending magnets under the Pelletron are turned off, the beam can be passed through a short beam line, denoted as U-bend in Fig.1a. This so-called U-bend mode was used for commissioning purposes.

BEAM RECIRCULATION

Insufficient stability of the electron beam recirculation was the main obstacle at the R&D and commissioning stages. Frequently, the terminal voltage was dropping by tens or hundreds of kV, and the protection system was turning the beam off (“a beam trip”). Sometimes, the terminal voltage would go down to nearly zero, with the vacuum pressure in the tubes increasing by several orders of magnitude and with electromagnetic waves often damaging the equipment (“a full discharge”).

Most of these events result from a charge accumulation on the tube ceramic, coming from lost electrons, and following partial discharges in the acceleration gaps. These discharges occur all the time, with frequency dependent on the tube voltage gradient and amount of beam loss. By itself, a discharge of a single gap cannot significantly change the overall voltage distribution. The structure of the Pelletron column contains large aluminium discs, called separation boxes, which are connected every ~60 cm (2') to both tubes resistive dividers as well as to a column resistive divider. When only one of 42 gaps contained between neighbouring separation boxes is discharged, the effect on the voltage outside this portion of the tube is negligible. However, with some probability a plasma plume from such discharges can also shorten one or several neighbouring gaps. If the unaffected portion of the tube is capable of holding the entire voltage, the gaps are charged up again, and the beam does not trip. If the envelope modification resulting from the altered voltage distribution is large but induces a beam loss only somewhere outside of the Pelletron, the protection system interrupts the beam and normal operation can be restored in a matter of seconds. Otherwise, the entire tube shortens, causing a full discharge.

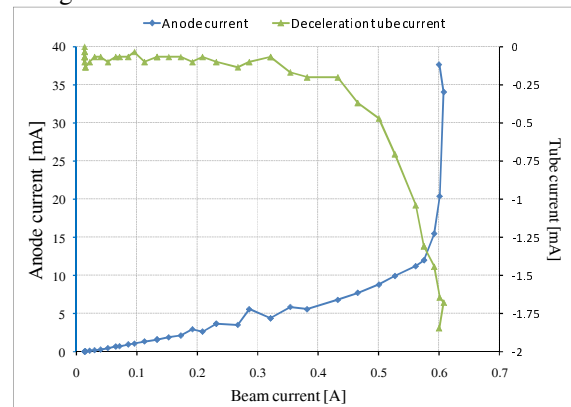


Figure 2. Anode current and changes in the deceleration tube current as functions of the beam current. Full line; ion clearing mode (December 31, 2011.).

Several steps allowed making the cooler an operational system.

- Development of an effective gun and collector with parameters well above operational requirements. The maximum current achieved and the typical relative beam loss were, correspondingly, 2.6 A and $2 \cdot 10^{-6}$ on

a low-energy test bench, 1.8 A and $1.2 \cdot 10^{-5}$ in the U-bend mode at 4.3 MeV, and 0.6 A and $1.8 \cdot 10^{-5}$ in the full line (Fig.2). The higher beam loss in longer systems is attributed to electron scattering on the residual gas and Intra Beam Scattering (IBS) [9].

- Decreasing the beam loss to the tubes, primarily by tuning the beam envelope in the deceleration tube to transport out of the Pelletron all electrons escaping from the collector. It was found that if the current of resistive dividers of either tube changes by more than $\sim 1 \mu\text{A}$, the frequency of beam trips increases in accordance with the discharge model explained above.
- Increasing the total length of the accelerating tubes by 1/5 improved dramatically the recirculation stability at 4.3 MV (operation voltage), in accordance with the logic of the previous paragraph. Note that in a test recently performed at much lower energy, 1.6 MeV, no single beam trip or full discharge have been observed [10].
- Adjusting the beam envelope in the acceleration tube to keep the beam core far from the tube electrodes in the time of the beam trips. It made a difference in preventing full discharges originating in the acceleration tube.
- Protection of the deceleration tube from irradiation in the time of beam trips by using optics with high dispersion in the return line.
- Fast protection circuitry, turning the beam off in $1 \mu\text{s}$ after detecting a Pelletron voltage drop of more than 5 kV or other abnormal conditions.

The implementation of these measures allowed operating typically with only several beam trips per day and full discharges as rare as once a year.

ELECTRON COOLING IN OPERATION

Since 2005, the Recycler Electron cooler is used in operation around the clock to accumulate antiprotons in the Recycler and prepare them for shots to the Tevatron. A typical stacking cycle is shown in Fig.3. Every 40-50 minutes, $\sim 25 \cdot 10^{10}$ antiprotons are transferred from the Accumulator into a free longitudinal space in the Recycler ring and then are merged with the main stack. The stack length stays constant all the time to minimize the longitudinal emittance dilution. After reaching the target stack size, antiprotons are aggressively cooled and transferred into the Main Injector for acceleration and injection into the Tevatron.

The manipulation of the electron beam is different for these two stages. During accumulation, the emphasis is on preserving a good life time while maintaining reasonable antiproton emittances. For that purpose, the electron beam is kept at 0.1 A and at a constant 2 mm offset (propagating in the cooling section parallel to the axis of the antiproton beam). Recently, adding a small-amplitude helical motion of the electron beam was found to be beneficial as well.

During the stage of final preparation of bunches and their transfer out of the Recycler, the strength of cooling

is increased to the level where the antiproton phase density comes close to an instability threshold. The helix is removed; the electron beam is brought “on axis” (i.e. position concentric with the antiproton beam); during the summer of 2011, in addition the beam current was increased to 0.2 A in the ion clearing mode (see below).

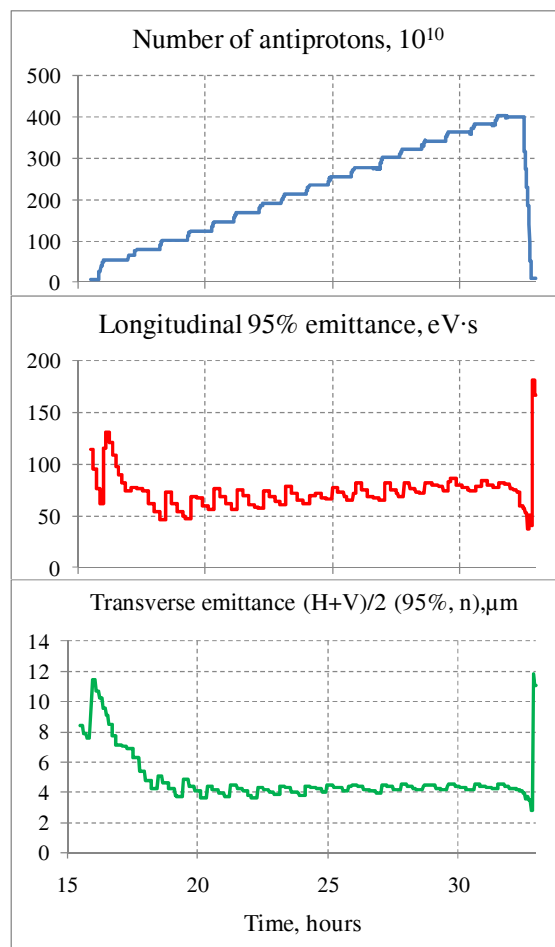


Figure 3. Typical cycle of accumulation of antiprotons in the Recycler ring and following extraction. June 17-18, 2011. Electron beam was kept at 0.1 A, shifted by 2 mm from the axis except until right before extraction, when it was switched to 0.2 A in ion clearing mode and moved on axis. The average life time was 256 hours, and initial luminosity in the Tevatron was $408 \cdot 10^{30} \text{ cm}^{-2} \text{ s}^{-1}$.

This procedure allows limiting the antiproton loss related to the final life time in the Recycler to 3-6% while increasing the beam brightness to the threshold determined by the capability of the Recycler transverse dampers. A significant progress to the accumulation rate and the life time resulted, in part, from enhancing electron cooling.

OPTIMIZATION OF COOLING

Details about the quality of the electron beam and strength of cooling are obtained from ‘drag rate’ measurements by a voltage jump method [11] similar to the one used at the early age of electron cooling [12]: a

“pencil” coasting antiproton beam is cooled to an equilibrium, the electron energy is changed by a jump, and the rate of change of the mean value of the antiproton momentum is recorded while the antiprotons are dragged toward the new equilibrium. If the momentum spread remains small in comparison with the difference between the two equilibriums, this ‘drag rate’ is equal to the longitudinal cooling force.

The results can be compared with the classical cooling model [13] ignoring the contribution of the magnetic field. In the simplified case of a constant Coulomb logarithm L_c , the formula can be expressed as [14]

$$F_{Lz}(\Delta p_p) = F_0 \int_0^{\frac{\Delta p_p}{p_1}} \frac{e^{-u^2} u^2}{u^2 + \left(\frac{\Delta p_p}{p_2}\right)^2} du \quad (2)$$

which parameters are related to the lab-frame electron beam properties as follows:

$$p_1 = \delta W_e \cdot \sqrt{2} \frac{M_p}{\beta m_e c}; \quad p_2 = \vartheta_i \cdot \sqrt{2} \gamma^2 \beta c M_p;$$

$$F_0 = \frac{n_{el}}{\vartheta_i^2} \cdot \frac{2}{\sqrt{\pi}} \cdot \frac{4\pi \cdot e^4 \eta_{CS} \cdot L_c}{m_e c^2 \gamma^3 \beta^2}$$

where θ_i is the 1D r.m.s. electron angle in the cooling section, δW_e the r.m.s. energy spread of the electron beam, n_{el} the electron density in the lab frame, M_p the proton mass, η_{CS} the portion of the ring occupied by the cooling section, and $p_e = \gamma \beta m_e c$ the electron beam momentum. Graphically Eq.(2) is presented in Fig.4. If the cooling force is measured near its maximum, it depends on the transverse electron angles approximately as θ_i^{-2} and can be used to estimate changes in the angle.

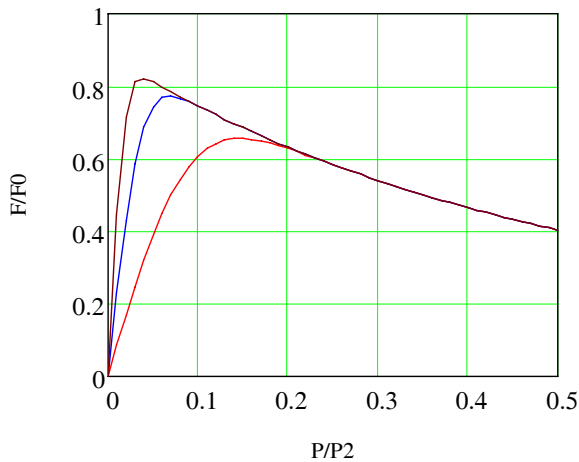


Figure 4. Normalized cooling force calculated with Eq.(2) as a function of $\Delta p_p/p_2$ for three ratios of p_2/p_1 : 10 (red), 25 (blue), and 50 (brown).

Results of the ‘drag rate’ measurements performed at different currents throughout the cooler history are shown in Fig. 5.

Electron cooling

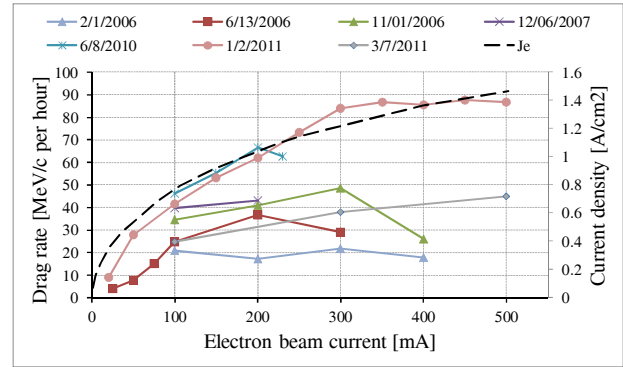


Figure 5. Cooling force as a function of the beam current measured on axis at various dates with a 2 kV voltage jump. The current density calculated at the beam center (dashed curve) is shown for comparison.

The significant enhancement of the cooling force presented in Fig.5 came mainly from three improvements that decreased the electron angles in the cooling section.

First, focusing was optimized by adjusting the corrector quadrupoles based on drag rate measurements at the electron beam periphery [15].

Second, a beam-based procedure for aligning the magnetic field in the cooling section was developed. The cooling section consists of 10 two-meter long solenoid modules, which are rigid but move with respect to one another when the tunnel deforms or the temperature changes. Compensation of the resulting transverse fields was made by adjusting 10 pairs of dipole correctors in each module. For this, a special electron trajectory was created that passed on axis for the module being optimized and with a large offset through the other parts of the cooling section. The cooling force measured in such configuration is determined mainly by the module with the beam on axis, and the transverse fields were adjusted module-by-module to maximize the force. For optimum performance, such optimization needs to be performed a couple times a year.

Finally, the electron angles were found to be affected by ions created by the electron beam and captured by its space charge. With no ion clearing mechanisms, the ion density would increase until reaching the electron one. At the neutralization factor of $\eta \sim 1$, the focusing effect from ions is a factor of $\gamma^2 \sim 100$ higher than defocusing from the beam space charge, thus an effective ion clearing is required.

All capacitive pickups monitoring the beam position in the cooler (BPMs) have a negative DC offset on one of their plates, while the other plate is DC grounded. The resulting electric field removes ions in the vicinity of each BPM. The neutralization time (17 sec for 0.3 nTorr of hydrogen) is much longer than the time for a thermal – velocity H_2^+ ion to fly ~ 5 m between two neighbouring BPMs, ~ 3 ms, and, therefore, clearing with the electric field in BPMs should be effective. However, significant size variations of both the electron beam and the vacuum pipe along the beam line create local potential minimums that prevent ions from travelling to the clearing field in

the BPMs. Also, solenoidal lenses providing focusing in the beam line create additional barriers for ions.

While this danger was realized at the design stage, the hope was that the focusing effect of the ion background would be mainly linear and, therefore, could be compensated by adjusting the lens settings. Indeed, the cooling properties of the electron beam were found good enough for what is the standard operation mode, at $I_e = 0.1$ A. However, cooling efficiency peaked at 0.1 – 0.2 A and decreased at higher currents while it is supposed to be monotonically increasing with I_e . Transverse scans of drag rates (Fig.6a) revealed that at $I_e = 0.3$ A only three narrow areas provide significant drag rates. This profile corresponds to high-order focusing perturbations that cannot be corrected by adjusting solenoidal lenses and quadrupoles.

The remedy to decrease the average ion concentration was found to be periodic interruptions of the electron beam. In the potential well created by electrons, ions gain the kinetic energy of up to 10 eV (at $I_e = 0.3$ A).

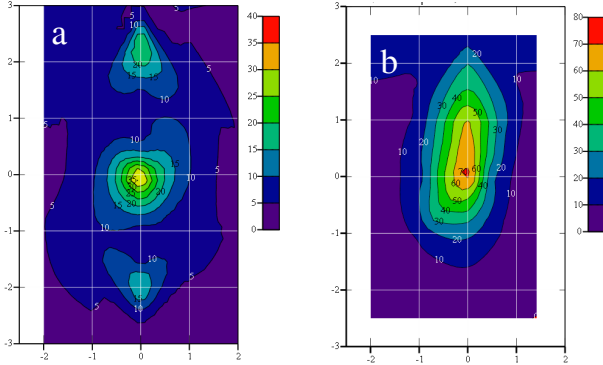


Figure 6. Contour plot of drag rates without (a) and with (b) ion clearing by beam interruptions. Voltage jump of 2 kV, $I_e=0.3$ A. In the mode with ion clearing, the interruption frequency was 100 Hz. Contour levels are in MeV/c/hr. Note the difference in scales.

Thus, if the electron beam is abruptly turned off, an H_2^+ ion reaches the vacuum pipe in 1-2 μ s. The capability of interrupting the electron current for 1 – 30 μ s with a frequency up to $f_{int} = 100$ Hz was implemented in the electron gun modulator in 2009 [16].

Dependence of the cooling force measured at 1mm offset on the interruption frequency is shown in Fig. 6. The results can be compared with the following greatly simplified model.

a. The beam space charge outside of the Pelletron tubes is relatively small, so that the envelope electron angle in the cooling section changes linearly with variation of the beam current and the offset r , $\Delta\alpha = k_{sc} \cdot r \cdot \Delta I_e$. According to OptiM [17] simulations, the coefficient $k_{sc} \approx 1$ rad/A/m.

b. The effect of accumulated ions is similar,

$$\Delta\alpha_i = k_{sc} \cdot r \cdot \Delta I_e \cdot \delta \cdot \eta \cdot \gamma^2 \quad (3)$$

where $\delta < 1$ is a fitting coefficient representing that ions can be accumulated only in a portion of the

Electron cooling

beam line, far from clearing fields of BPMs.

c. Neutralization drops to zero at the interruption, increases linearly with time until reaching an equilibrium at some value η_0 , and then stays constant:

$$\eta(t) = \begin{cases} t / \tau_c, & t \leq \tau_0 \\ \eta_0, & t > \tau_0 \end{cases} \quad \tau_c = \frac{1}{n_a \sigma_i \beta c}; \quad \tau_0 = \eta_0 \tau_c \quad (4)$$

where n_a is the atom density and σ_i is the ionization cross section of hydrogen.

d. The cooling force F_c changes with the additional envelope angle introduced by neutralization as

$$F_c = \frac{F_0}{1 + (\Delta\alpha_i / \alpha_0)^2}, \quad (5)$$

where α_0 and F_0 are the rms angle and drag force at optimum focusing.

e. The measured drag rate F_d is the cooling force averaged over the period between interruptions (assuming that the pencil antiproton beam is sensitive mainly to the electron angles in the location of its center)

$$F_d = f_{int}^{-1} \int_0^{1/f_{int}} F_c(t) dt \quad (6)$$

Calculation with Eq. (3) - (6) for $\delta = 0.5$, $\eta_0 = 0.02$, and $F_0 = 73$ MeV/c/hr, shown as a dashed line in Fig. 7, follows well the experimental data.

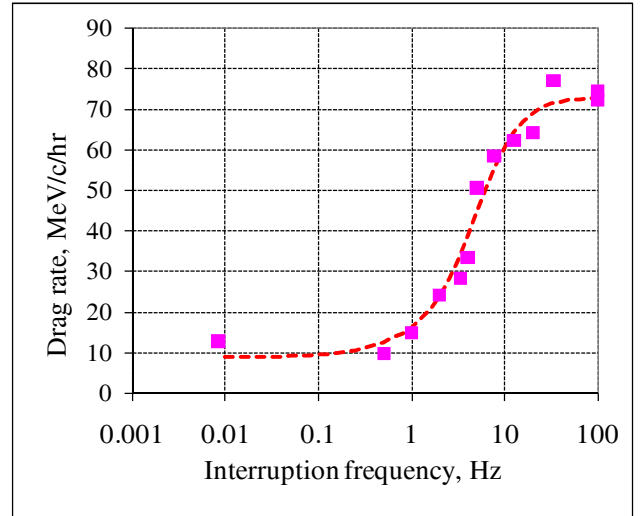


Figure 7. Drag rate as a function of the interruption frequency f_{int} for $I_e = 0.3$ A and separation between beams of 1 mm. January 2, 2011. The interruption pulse was 2 μ s. Focusing was optimized on axis at 20 Hz. The squares represent the data, and the line is the model.

Clearing ions by beam current interruptions significantly increased the area of the electron beam cross section with good cooling (Fig. 6b) as well as improved the drag rate measured on axis at higher electron currents

(Fig. 5). The latter result is probably related to the finite transverse size of the “pencil” antiproton beam in the measurements.

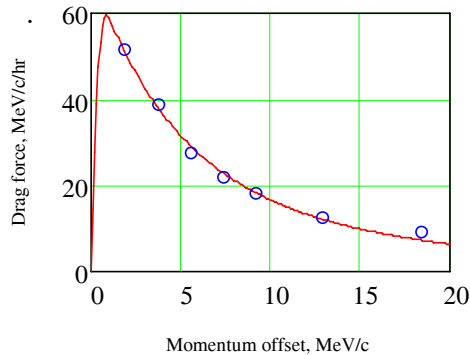


Figure 8. Drag rate as a function of momentum offset. $I_e=0.1A$, focusing is optimized for ion clearing, 100 Hz. The circles are data, and the solid line is a calculation with Eq.(2) at $\theta_e=80\mu\text{rad}$, $\delta W_e=200\text{eV}$, $L_c=9$. January 4, 2011.

The cooling force measured at different momentum offsets with ion clearing is presented in Fig. 8 for $I_e=0.1A$. Note that attempts to measure the force at momentum offsets lower than shown there (3.8 MeV/c) were unsuccessful because the longitudinal distribution moved too quickly toward the new equilibrium in order to reliably extract the value of the force. As a result, this set of measurements cannot give a reasonable estimation of the electron energy spread.

It is interesting to compare the angle in the cooling section from the fit to the data of Fig.8 with independent estimations of various components (Table 2). Each component is shown averaged over the electron beam size of 2 mm (radius), cooling section length, and time. The total, showing the components summed in quadrature, is close to that estimated from the drag rate measurements.

Table 2. Contributions to the total electron angle in the cooling section. Shown values are 1D, rms.

Effect	Angle, μrad	Method of evaluation
Thermal velocities	57	Calculated from the cathode temperature
Envelope mismatch	~50	Comparing resolution of tuning and simulations
Dipole motion (above 0.1 Hz)	~35	Spectra of BPMs in the cooling section
Dipole motion (field imperfections)	~50	Magnetic field measurements
Non-linearity in lenses	~20	Trajectory response to dipole kicks
Ion background	< 10	Cooling measurements
Total	~100	Summed in quadrature

CONCLUSION

Electron cooling was an effective tool for increasing the luminosity of the Tevatron complex. The maximum strength of cooling was noticeably increased in the course of Run II, with the main improvements being tuning the beam envelope with quadrupoles, aligning the magnetic field in the cooling section, and removing ions captured by the beam.

ACKNOWLEDGEMENTS

The success of electron cooling at Fermilab came as a result of efforts of many people, whose list would not fit into this paper. Authors are thankful to all of them for their dedicated work and for the joy working as a great team.

REFERENCES

- [1] Fermilab Recycler Ring Technical Design Report, FERMILAB-TM-1991, 1996
- [2] S. Nagaitsev et al., Phys. Rev. Lett. 96, 044801 (2006)
- [3] FERMILAB-TM-2061, Oct 1998. 91pp., edited by J.A. MacLachlan.
- [4] N. Dikansky et al., Electron beam focusing system, in FERMILAB-TM-1998 (1996)
- [5] A.Burov et al., PRST – AB, 094002 (2000)
- [6] Pelletrons are manufactured by the National Electrostatics Corporation, www.pelletron.com
- [7] A. Sharapa et al., NIM-A 417 (1998) 177
- [8] L.R. Prost and A. Shemyakin, Proc. of PAC'05, Knoxville, USA (2005) p.2387
- [9] A. Burov et al., Proc. of COOL'05, Galena, USA (2005), p. 159, also available as FERMILAB-CONF-05-462-AD
- [10] L. R. Prost et al., Proc. of PAC'11, New York, USA (2011), WEP113
- [11] L. Prost et al., Proc. of HB2006, Tsukuba, Japan, May 29-June 2, 2006, WEAY02
- [12] G.I.Budker et al., Preprint IYaf 76-32 (1976), <http://cdsweb.cern.ch/record/118046/files/CM-P00100706.pdf>
- [13] Ya.S. Derbenev and A.N. Skrinsky, Particle Accelerators, 8, p.1 (1977)
- [14] A. Shemyakin and L.R. Prost, Proc. of APAC'07, Indore, India (2007), TUPMA094
- [15] A. Shemyakin et al., Proc. of PAC'09, Vancouver, Canada (2009), TU6PFP076
- [16] A. Shemyakin et al., Proc. of IPAC'10, Kyoto, Japan (2010), MOPD075
- [17] V. Lebedev, “OptiM”, at <http://www-bdnew.fnal.gov/pbar/organizationalchart/lebedev/OptiM/optim.htmA>.